Occurrence of elves and lightning during El Niño and La Niña

Y. J. Wu,[1] A. B. Chen,[2] H. H. Hsu,[3] J. K. Chou,[1] S. C. Chang,[1] L. J. Lee,[1] Y. J. Lee,[1] H. T. Su,[1] C. L. Kuo,[1] R. R. Hsu,[1] H. U. Frey,[4] S. B. Mende,[4] Y. Takahashi,[5] and L. C. Lee[6]

Received 1 December 2011; revised 9 January 2012; accepted 17 January 2012; published 10 February 2012.

[1] We analyzed the ISUAL-FORMOSAT2 elves, the LIS-TRMM lightning, the sea surface temperature (SST), and the El Niño southern oscillation (ENSO) indices (the Niño 3.4 Index and the Southern Oscillation Index - SOI) in the period between June 2005 and May 2010 to explore the impacts of ENSO on the occurrences of the mesospheric elves and the troposphere lightning. The standardized anomalies of the elve and the lightning occurrence densities are used to quantify the deviation of the elve and lightning occurrences during an ENSO event. The areas in the ENSO-sensitive western Pacific, central Pacific and Tahiti regions with a significant event anomaly are taken to be the impact indicators of ENSO. Also the SOI is used to examine the correlation of the temporal intensity variation between ENSO, elve and lightning. The results indicate that elve shows clear responses to ENSO with a correlation over 0.6 in the coastal and the oceanic regions. The lightning occurrence is responsive to ENSO in the oceanic regions, but shows a low correlation in the coastal regions, due the overwhelming influence of the landmass. Therefore, between elve and lightning as proximity indices of ENSO, elve has a broader applicable geographic range. However, elve is known to be the mesospheric luminous manifestations of the high-peak-current lightning, and the response of the intense lightning to ENSO would be similar to that of the elve. Hence, alternatively, the intense lightning can also be used as an indicator of ENSO. **Citation:** Wu, Y. J., et al. (2012), Occurrence of elves and lightning during El Niño and La Niña, *Geophys. Res. Lett.*, *39*, L03106, doi:10.1029/2011GL049831.

1. Introduction

[2] Transient luminous events (TLEs), which include sprites, elves, halos, and electric jets, are lightning induced large-scale optical transient phenomena occurring between the troposphere and the lower ionosphere [*Pasko*, 2010, and references therein]. To better understand these atmospheric optical events, Imager of Sprite and Upper Atmospheric Lightning (ISUAL) onboard the FORMOSAT-2 (FS2) has carried out a global survey of TLEs since July 2004. The results show that the elves induced by intense lightning with peak current exceeding 80kA are the dominant type of TLEs and account for ~80% of the TLE events [*Chen et al.*, 2008; *Kuo et al.*, 2007]. The distribution of TLEs also exhibits a preferred latitudinal pattern, with most of the TLEs occurring in the Intertropical Convergence Zone (ITCZ)/South Pacific Convergence Zone (SPCZ) during the local summer and near the cold fronts of the mid-latitude storms during the local winter [*Lee et al.*, 2010].

[3] The El Niño Southern Oscillation (ENSO) is known to be the longitudinal large scale phenomenon that influences the location and the intensity of the Walker Circulation, the sea surface temperature, and the wind in the Pacific region [e.g., *Walker*, 1923; *Wyrtki*, 1975] as well as the global climate through teleconnection patterns [e.g., *Wang et al.*, 2000; *Camberlin et al.*, 2001]. Recently ENSO was also documented as an important player in driving the lightning activity. For example, *Williams* [1992] shown that the lightning flash rate varies with the surface temperature; notably, the interannual lightning rate exhibits surges with the phase of ENSO. *Sátori et al.* [2009] demonstrated that the lightning occurrence is more frequent during the cold phase (La Niña) than that during the warm phase (El Niño) for the Pacific and other oceanic regions. *Chronis et al.* [2008] noted that there is a lightning occurrence enhancement during the warm (El Niño) phase of the central Pacific and the eastern Indian Oceans, while for the southwestern Pacific Ocean and the coasts of Brazil/South Africa the enhancement occurred during the cold (La Niña) phase. These results indicate that the subtle link between the lightning occurrence and the ENSO phenomenon are tied both locally and globally.

[4] In this study we compare the ISUAL-FS2 elve data, the LIS-TRMM lightning data, the NOAA Optimum Interpolation sea surface temperature (SST), the Niño 3.4 index and the Southern Oscillation Index (SOI), to clarify the impacts of ENSO events on the elves near the lower ionosphere boundary. The data and the analysis methods are shown in Section 2. The variations of elve and lighting occurrences during the ENSO events in the western Pacific, the central Pacific, and the Tahiti regions are presented in Section 3. The quantitative correlation between ENSO, elves and lightning is discussed in Section 4, and the summary is highlighted in Section 5.

2. Data and the Analysis Methods

[5] The elve and the lightning data used in this study are recorded by the ISUAL/FS2 [*Chern et al.*, 2003; *Chen et al.*, 2012] and the LIS-TRMM [*Christian et al.*, 1999; *Boccippio et al.*, 2000] between June 2005 and May 2010 accordingly. To normalize the regional viewing time non-uniformity, the

[1]Department of Physics, National Cheng Kung University, Tainan, Taiwan.
[2]Institute of Space, Astrophysical and Plasma Sciences, National Cheng Kung University, Tainan, Taiwan.
[3]Research Center for Environmental Change, Academia Sinica, Taipei, Taiwan.
[4]Space Sciences Laboratory, University of California, Berkeley, California, USA.
[5]Department of Cosmosciences, Hokkaido University, Sapporo, Japan.
[6]Institute of Space Science, National Central University, Jungli, Taiwan.

0094-8276/12/2011GL049831

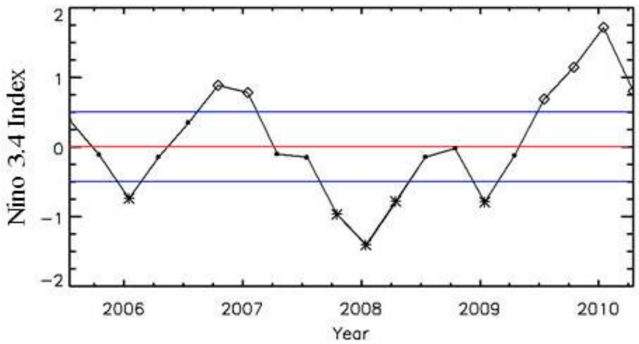

Figure 1. Nino 3.4 index for the 20 seasons between JJA 2005 and MAM 2010; hollow-squares - El Niño events and stars - La Niña events.

occurrence density as the number of events/flashes per km square per observation time during a year (#/km^2/year) is used [*Christian et al.*, 2003] to quantify the elve/lightning occurrence [*Chen et al.*, 2008]. The occurrence density in 0.5° × 0.5° square grid and is further resampled in 2.5° square grid. The *event occurrence rate* for a grid can be obtained by multiplying the grid occurrence density with the grid area. In this work, only elves occurring over the regime between 30°S to 30°N are analyzed, since it is the only area that ISUAL has a complete year-round coverage, though with some minor gaps [*Chen et al.*, 2008]. Hence to perform a proper comparison of the elve and the lightning data, the lightning that fall in the ISUAL observational gaps are removed and the LIS-TRMM lightning data used here are gap-corrected.

[6] The Niño 3.4 Index is the standard quantity in identifying the sea surface temperature anomaly (SSTA) 120°W-170°W and 5°S-5°N region [*Trenberth*, 1997]. When the Niño 3.4 Index is greater (less) than or equal to +0.5 (−0.5), a warm (cold) event is identified. As shown in Figure 1, the data scope includes 20 seasons; six are warm and five are cold ENSO events.

[7] Before exploring the impact of an ENSO event on the elve and the lightning occurrences, seasonal effects [e.g., *Lee et al.*, 2010; *Sato et al.*, 2008] must be excluded. The mean seasonal occurrence density is subtracted from the original occurrence density to obtain the occurrence density for the season i, x_i. Furthermore, the standardized anomaly is used to characterize the degree of responses of elve/lightning to ENSO, to objectively compare the number of *standard deviations* the anomaly departed from the normal over different regions. The standardized anomaly of the occurrence density for a grid point in season i is $Z_i = \frac{x_i - \mu}{\sigma/\sqrt{n-1}}$, where μ is the expectation value, and $\sigma/\sqrt{n-1}$ is the corrected standard deviation for a small sample size (n < 30) [*Federighi*, 1959].

[8] From the student-t distribution, the absolute standardized anomaly must be greater than 1.729 to have a 90% confidence level for a sample size of 20 [*Federighi*, 1959]. For a season with an absolute standardized anomaly exceeds 1.729; the seasonal variation is termed as "significant increase" or "significant decrease" respectively for positive or negative values.

[9] To find the features of elve/lightning occurrence during ENSO, the average standardized anomaly of the event occurrence density during the cold and the warm phases $\bar{Z}_{warm} = \frac{\sum_{warm} Z_i}{n_{warm}}$ and $\bar{Z}_{cold} = \frac{\sum_{cold} Z_i}{n_{cold}}$ are respectively computed. Figures 2a and 2b exhibit the average standardized anomalies of the elve occurrence density during the warm and the cold phases, the pink-shaded grids denote the regions where the occurrence of elve increases significantly, while the blue-shaded grids mark the regions where the occurrence of elve decreases significantly. The same procedure is also applied to the analysis between lightning and SST; the standardized SSTA is shown as the contouring-lines in all the panels of Figure 2, and the corresponding lightning anomalies are presented in Figures 2c and 2d. The warm SST regions congregate into a tongue-like area along the equatorial central and eastern Pacific regions, which is flanked by a horseshoe-like cold SST region on both sides. The anomalies are in reverse during the cold phases. These patterns resemble that of the recently documented El Niño Modoki or the central Pacific El Niño [e.g., *Ashok et al.*, 2007; *Yeh et al.*, 2009].

3. Elve and Lightning Occurrences in the ENSO-Sensitive Regions

[10] For the correlation between ENSO and the elve/lightning occurrence, three ENSO-sensitive regions are studied; the central Pacific region (165°E ∼ 165°W, 10°S ∼ 10°N) in the positive pole of the El Nino Modoki [*Ashok et al.*, 2007], the western Pacific region (130°E ∼ 150°E, 10°S ∼ 20°N) in the negative pole of the El Niño Modoki [*Ashok et al.*, 2007], and the Tahiti region (165°W ∼ 135°W, 25°S ∼ 5°S), which is a region well-known for its sensitive response to ENSO [e.g., *Sátori et al.*, 2009] .The occurrences of elve and lightning are sporadic in the other remaining ENSO sensitive eastern Pacific regions, thus these regions are excluded in this study.

[11] To quantify the correlation of the elve and the lightning occurrences on ENSO, the percentage of the area with a significant occurrence density anomaly is listed in Table 1. For the central Pacific region, a large area is found to have significant elve/lightning occurrence increase during the warm phase, while they are suppressed during the cold phase over a wide area. The area with an enhanced elve occurrence during the warm phase is higher than that for the lightning in the positive pole of the El Niño Modoki. For the western Pacific region, the negative pole of the El Niño Modoki, both the elve and the lightning occurrences are enhanced over a wide area during the cold phase. During the warm phase though, elve and lightning occurrences show no noticeable reduction.

[12] For the Tahiti region, both elve and lightning occurrences are enhanced during the cold phase but are suppressed during the warm phase. The suppression of the lightning occurrence during the warm phase is more pronounced than that for the elve. Also, the changes in the elve and lightning occurrences did not coincide with the variation of the SST. The lightning occurrence is responsive to ENSO but not to SST in the Tahiti region was also reported by *Sátori et al.* [2009].

4. Quantifying the Correlation Between Elve, Lightning and ENSO

[13] In the study regions, both the elve and the lightning occurrences show responses to the ENSO events. In this

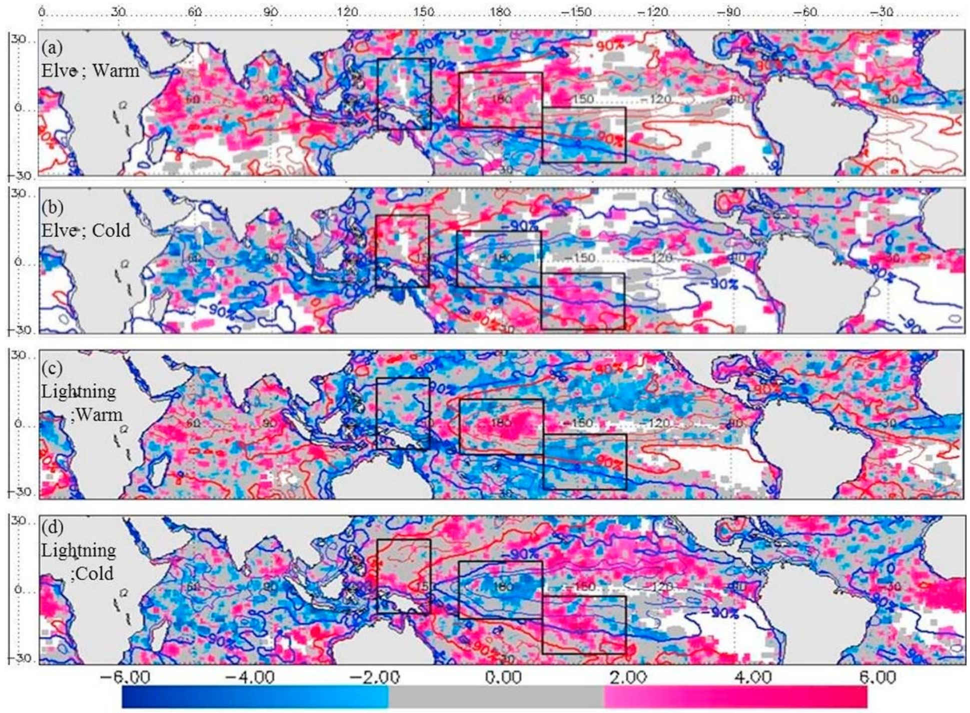

Figure 2. The average standardized anomalies of the elve and lightning occurrence densities during ENSO: (a and c) the warm phase and (b and d) the cold phase. Color codes: pink shaded, area with significant occurrence increase; blue shaded, area with significant occurrence decrease; gray shaded, area with no significant occurrence changes; blue (red) lines, isopleths of the SSTA; blocked areas (left to right), the western Pacific, the Pacific and the Tahiti regions.

section, an elve/lightning ENSO index is constructed to examine the temporal correlation between the elve/lighting occurrence density and the intensity of ENSO. To properly account for the seasonal elve occurrence, the monthly variation SOI is re-sampled to become a seasonal data set. The ENSO indices for elve and lightning at the two comparative pairing regions: the western Pacific region versus the central Pacific region and the Tahiti region versus the central Pacific are defined as:

$$\mathrm{I}_{\mathrm{i;W,C}}^{\mathrm{elve(lightning)}} \equiv \mathrm{Z}_{\mathrm{i;W}}^{\mathrm{elve(lightning)}} - \mathrm{Z}_{\mathrm{i;C}}^{\mathrm{elve(lightning)}},$$

and

$$\mathrm{I}_{\mathrm{i;T,C}}^{\mathrm{elve(lightning)}} \equiv \mathrm{Z}_{\mathrm{i;T}}^{\mathrm{elve(lightning)}} - \mathrm{Z}_{\mathrm{i;C}}^{\mathrm{elve(lightning)}},$$

where $\mathrm{Z}_{\mathrm{i;W}}^{\mathrm{elve(lightning)}}$ is the standardized anomaly of elve (lightning) rate in the western Pacific region, whereas $\mathrm{Z}_{\mathrm{i;C}}^{\mathrm{elve(lightning)}}$ and $\mathrm{Z}_{\mathrm{i;T}}^{\mathrm{elve(lightning)}}$ are those for the central Pacific and the Tahiti regions.

[14] Figure 3 (top) shows the seasonal variation of $\mathrm{I}_{\mathrm{i;W,C}}^{\mathrm{elve}}$ (red line), $\mathrm{I}_{\mathrm{i;W,C}}^{\mathrm{lightning}}$ (blue line) and SOI (black line) between JJA 2005 and MAM 2010 for the western Pacific and the central Pacific pairing regions. The respective correlation for $\mathrm{I}_{\mathrm{i;W,C}}^{\mathrm{elve}}$ and $\mathrm{I}_{\mathrm{i;W,C}}^{\mathrm{lightning}}$ with SOI are 0.63 and 0.36. The variations of the ENSO indices for the Tahiti and the central Pacific pairing regions are in Figure 3 (bottom); while the respective correlation with SOI are 0.68 and 0.63 for $\mathrm{I}_{\mathrm{i;T,C}}^{\mathrm{elve}}$ and $\mathrm{I}_{\mathrm{i;T,C}}^{\mathrm{lightning}}$. The correlation between the elve ENSO index and the SOI are over 0.6 for both pairing regions.

[15] The disparity response of elve and lightning to ENSO may lie in the land-ocean asymmetry for these two types of events. The occurrence ratio between the land and the oceanic elves is nearly 1 to 1 [*Chen et al.*, 2008], while that for the lightning is close to 10 to 1 [*Christian et al.*, 2003]. The

Table 1. The Area With a Significant Enhancement or Suppression of Elve/Lightning Occurrence During ENSO in the Central Pacific, the West Pacific and the Tahiti Regions[a]

Region	Event	Warm Phase (El Niño)		Cold Phase (La Niña)	
		Enhance Area	Reduce Area	Enhance Area	Reduce Area
Central Pacific	elve	**41.1%**	1.9%	3.1%	**24.5%**
	lightning	**34.9%**	12.1%	6.3%	**33.9%**
West Pacific	elve	13.4%	12.9%	**21.7%**	10.8%
	lightning	6.4%	15.7%	**20.3%**	6.8%
Tahiti	elve	6.5%	**21.6%**	**35.2%**	7.1%
	lightning	2.0%	**44.7%**	**43.0%**	4.1%

[a]Bold indicates areas with a more significant enhancement or suppression of elve/lightning occurrence during ENSO.

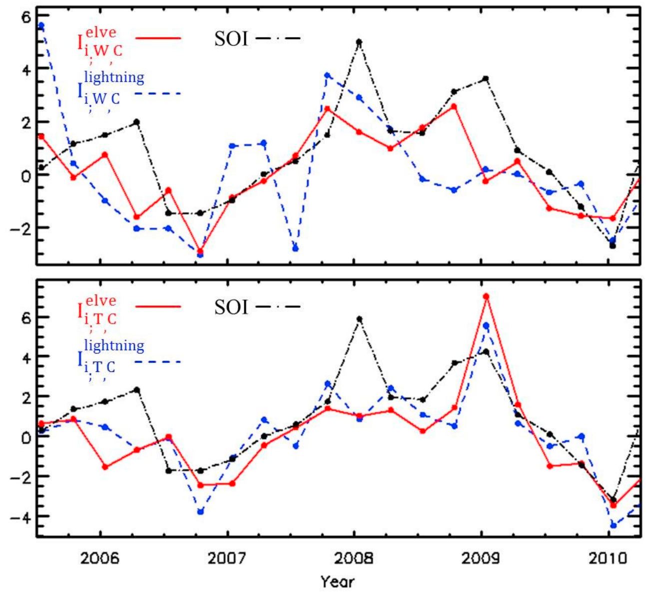

Figure 3. $I^{elve}_{i;W(T),C}$ (red line), $I^{lightning}_{i;W(T),C}$ (blue line) and SOI (black line) for (top) the western Pacific and the central Pacific pair and (bottom) the Tahiti and the central Pacific pair.

western Pacific region is in the coast and the land may have exerted more influence on $I^{lightning}_{i;W,C}$ than ENSO. This may also explain why the correlation between $I^{lightning}_{i;W,C}$ and the SOI is low. Both the central Pacific and the Tahiti regions are oceanic areas, thus the correlation between ENSO and $I^{lightning}_{i;T,C}$ can be readily shown.

5. Discussion and Conclusions

[16] We analyzed the ISUAL-FS2 elve and the LIS-TRMM lightning data to show that the elve and lightning occurrences are sensitive to ENSO events. Elve and lightning occurrence densities vary in phase with SST in the central Pacific and Western Pacific regions. In addition, the enhancement of elve occurrence during warm phases is particularly pronounced in the central Pacific region. The Tahiti region is also an ENSO sensitive region, although both the elve and the lightning occurrences were found to vary out of phase with the SST. Besides the target regions, Figure 2 indicate that elve and lightning occurrences in the west and the east shores of Indian Ocean, the west equatorial Africa, and the west coast of Africa around 20°N also have sensitive response to ENSO. Besides the target regions, these regions may also be good candidate regions for the studies of the ENSO effects.

[17] By applying a similar definition for SOI to elve and lightning occurrence rate, the correlations of the elve/lightning ENSO indices with SOI were both found to be over 0.6 for the central Pacific and the Tahiti regions. These results indicate that ENSO exerts significant impacts on the elve and the lightning occurrences in these two oceanic regions. In the western Pacific coastal region, the elve occurrence shows a clear response to the ENSO, but the response of the lightning is suppressed, due to the landmass effects. Therefore, between elve and lightning as indices of ENSO, elve has a broader applicable geographic range.

[18] Since elve is the mesospheric luminous manifestation of the high-peak-current (>60kA) intense lightning [*Barrington-Leigh et al.*, 2001], the response of the intense lightning to the ENSO should be similar that of the elve. Hence by monitoring lightning with sufficiently high peak currents using VLF sensors, the elve occurrence and the impact of ENSO can be monitored. Hence, the intense lightning is also a good indicator of ENSO.

[19] **Acknowledgments.** This work was supported in part by the National Science Council (NSC) and NSPO in Taiwan under grants NSC 100-2111-M-006 -002, NSPO-S-100010, NSC 100-2111-M-006 -001, and NSPO-S-100010. We thank NOAA/OAR/ESRL PSD for the NOAA_OI_SST_V2 data and LIS/TRMM for the lightning data.

[20] The Editor thanks two anonymous reviewers for their assistance in evaluating this paper.

References

Ashok, K., S. K. Behera, S. A. Rao, H. Weng, and T. Yamagata (2007), El Nino Modoki and its possible teleconnection, *J. Geophys. Res.*, *112*, C11007, doi:10.1029/2006JC003798.

Barrington-Leigh, C. P., U. S. Inan, and M. Stanley (2001), Identification of sprites and elves with intensified video and broadband array photometry, *J. Geophys. Res.*, *106*, 1741–1750, doi:10.1029/2000JA000073.

Boccippio, D. J., S. J. Goodman, and S. Heckman (2000), Regional difference in tropical lightning distribution, *J. Appl. Meteorol.*, *39*, 2231–2248.

Camberlin, P., S. Janicot, and I. Poccard (2001), Seasonality and atmospheric dynamics of the teleconnection between African rainfall and tropical sea-surface temperature: Atlantic vs. ENSO, *Int. J. Climatol.*, *21*, 973–1005, doi:10.1002/joc.673.

Chen, A. B., et al. (2008), Global distributions and occurrence rates of transient luminous events, *J. Geophys. Res.*, *113*, A08306, doi:10.1029/2008JA013101.

Chen, A. B., et al. (2012), Sensitivity degradation of ISUAL instruments and its impact on observations, *Terr. Atmos. Oceanic Sci.*, *23*, 71–83, doi:10.3319/TAO.2011.06.20.01(AA).

Chern, J. L., R. R. Hsu, H. T. Su, S. B. Mende, H. Fukunishi, Y. Takahashi, and L. C. Lee (2003), Global survey of upper atmospheric transient luminous events on the ROCSAT-2 satellite, *J. Atmos. Sol. Terr. Phys.*, *65*(5), 647–659, doi:10.1016/S1364-6826(02)00317-6.

Christian, H. J., et al. (1999), The Lightning Imaging Sensor, paper presented at 11th International Conference on Atmospheric Electricity, Am. Meteorol. Soc., Guntersville, Ala., 7–11 June.

Christian, H. J., et al. (2003), Global frequency and distribution of lightning as observed from space by the Optical Transient Detector, *J. Geophys. Res.*, *108*(D1), 4005, doi:10.1029/2002JD002347.

Chronis, T. G., S. J. Goodman, D. Ceci, D. Buechler, F. J. Robertson, J. Pittman, and R. J. Blakeslee (2008), Global lightning activity from the ENSO perspective, *Geophys. Res. Lett.*, *35*, L19804, doi:10.1029/2008GL034321.

Federighi, E. T. (1959), Extended tables of the percentage points of Student's t-distribution, *J. Am. Stat. Assoc.*, *54*, 683–688, doi:10.2307/2282546.

Kuo, C.-L., et al. (2007), Modeling elves observed by FORMOSAT-2 satellite, *J. Geophys. Res.*, *112*, A11312, doi:10.1029/2007JA012407.

Lee, L. J., et al. (2010), The controlling synoptic-scale factors for the distribution of the transient luminous events (TLEs), *J. Geophys. Res.*, *115*, A00E54, doi:10.1029/2009JA014823.

Pasko, V. P. (2010), Recent advances in theory of transient luminous events, *J. Geophys. Res.*, *115*, A00E35, doi:10.1029/2009JA014860.

Sato, M., Y. Takahashi, A. Yoshida, and T. Adachi (2008), Global distribution of intense lightning discharges and their seasonal variations, *J. Phys. D Appl. Phys.*, *41*, 234011, doi:10.1088/0022-3727/41/23/234011.

Sátori, G., E. Williams, and I. Lemperger (2009), Variability of global lightning activity on the ENSO time scale, *Atmos. Res.*, *91*, 500–507, doi:10.1016/j.atmosres.2008.06.014.

Trenberth, K. E. (1997), The definition of El Niño, *Bull. Am. Meteorol. Soc.*, *78*, 2771–2777, doi:10.1175/1520-0477(1997)078<2771:TDOENO>2.0.CO;2.

Walker, G. T. (1923), Correlation in seasonal variation of weather, VIII: A preliminary study of world weather, *Mem. Indian Meteorol. Dep.*, *24*, 75.

Wang, B., R. Wu, and X. Fu (2000), Pacific–East Asian teleconnection: How does ENSO affect East Asian climate?, *J. Clim.*, *13*, 1517–1536.

Williams, E. R. (1992), The Schumann resonance: A global tropical thermometer, *Science*, *256*, 1184–1187, doi:10.1126/science.256.5060.1184.

Wyrtki, K. (1975), Investigation of the EI Nino phenomenon in the Pacific Ocean, *Environ. Conserv.*, *2*, 281–282, doi:10.1017/S0376892900001806.

Yeh, S., J. Kug, B. Dewitte, M. Kwon, B. P. Kirtman, and F. Jin (2009), El Nino in a changing climate, *Nature*, *461*, 511–514, doi:10.1038/nature08316.

S. C. Chang, J. K. Chou, R. R. Hsu, C. L. Kuo, L. J. Lee, Y. J. Lee, H. T. Su, and Y. J. Wu, Department of Physics, National Cheng Kung University, Tainan 70701, Taiwan. (rrhsu@phys.ncku.edu.tw, htsu@phys.ncku.edu.tw)

A. B. Chen, Institute of Space, Astrophysical and Plasma Sciences, National Cheng Kung University, Tainan 70101, Taiwan.

H. U. Frey and S. B. Mende, Space Sciences Laboratory, University of California, 7 Gauss Way, Berkeley, CA 94720-7450, USA.

H. H. Hsu, Research Center for Environmental Change, Academia Sinica, 128 Academia Rd., Section 2, Nankang, Taipei 115, Taiwan.

L. C. Lee, Institute of Space Science, National Central University, 300 Jhongda Rd., Jungli, Taoyuan 3200, Taiwan.

Y. Takahashi, Department of Cosmosciences, Hokkaido University, Kita-10, Nishi-8, Kita-ku, Sapporo 060-0810, Japan.